ISSN 1330-3651 (Print), ISSN 1848-6339 (Online)
https://doi.org/10.17559/TV-20230203000316
Original scientific paper

Flexspline Deformation Analysis Depending on the Polymer Material Used in the Harmonic Drive Prototype

Jacek PACANA, Andrzej PACANA*

Abstract: Harmonic drives are traditionally made of steel by machining methods. Their advantages are the reason why attempts are made to use them in space vehicles or control systems. The next step is to test the feasibility of manufacturing these gears in space using rapid prototyping (RP) methods. Harmonic drives can be produced there from polymer materials because their load in space will be multiple lower. This article presents an analysis of the deformations of the flexspline performed by various rapid prototyping methods from different polymer materials. For the flexspline only deformed by the wave generator, no significant differences were observed between the materials used, but after loading, the most favourable results were obtained for PA 2200 polyamide. The results obtained for various polymer materials will contribute to further work on the design of the harmonic drives, which will be prepared using the RP methods in space.

Keywords: 3D printing; FDM, flexspline; harmonic drive; MEM; polymeric materials

1 INTRODUCTION

Harmonic drives are commonly used in robot and manipulator, control systems, and machine tool control. They are used mainly due to their high kinematic accuracy and small backlash [1-3]. Their important advantage is also the possibility of obtaining a large gear ratio at one stage. Today, thanks to new materials and manufacturing technologies [4-10], they are becoming more popular among the space industry [11-13]. The harmonic drive consists of a flexspline, a circular spline, and a wave generator. Models of harmonic drive components prepared for analysis are presented in Fig. 1. The solution most often used in practice was chosen, i.e. a cup-type flexspline, and a circular spline in the form of a ring, and a cam generator. These standard harmonic drives are available for sale from major manufacturers [14, 15]. These ready-made harmonic drives are designed to be high-power, made of steel, and are only available in specific sizes. However, such a high load capacity is not always required from harmonic drives, and its availability and the ability to easily produce its components are more important.

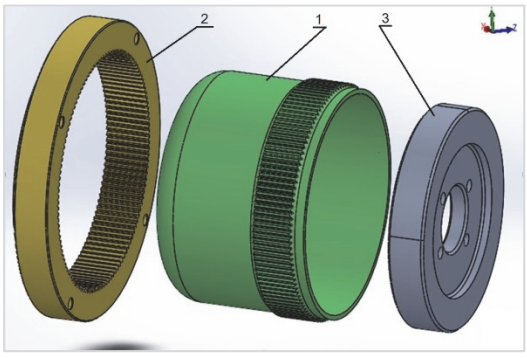

Figure 1 Models of harmonic drive components prepared by FEM numerical calculations; 1 - flexspline, 2 - circular spline, 3 - wave generator

New expectations regarding the use of harmonic drives in space devices have caused a significant increase of the requirements set for them so far. Harmonic drives were already used to propel Mars rovers and control the communication antennas of spacecraft, but they were standard steel structures [16, 17]. The costs of launching every kilogram into space are enormous, the harmonic drives should be as light as possible. Therefore, this research concerns harmonic drives that are much lighter because they are made of polymeric materials. When limiting the weight of the mechanism, you cannot forget its functionality and maintaining the required durability. Therefore, the article checks the suitability of selected polymer materials for the production of wave gear components. The selection of RP materials and methods included in the article took into account the possibility of production of wave gear components in space. The most loaded element of the harmonic drive is the flexspline. So, the deformation of the harmonic drives, under the influence of a cam generator was checked. For the calculations, models made of four different materials were adopted, which can be used in rapid prototyping methods. In further research work, functional prototypes will be made from the same materials and tested in research stands. The materials included in the analysis are used to produce models using additive methods. These technologies are based on a common method of transforming a continuous solid model into a set of discrete parallel layers of finite thickness. These layers are added to each other in sequence in the process of creating a physical model until the full element is created. The thickness of the layers directly affects the accuracy of the product, and depends on the chosen additive method. This way of producing machine components and their assemblies can be crucial in their production in pace. Thanks to the use of additive methods, it is also possible to create replacements for elements that have been damaged on a space station or a base on Mars. Copies of the destroyed machine components are then reproduced by reverse engineering (RE) methods without loss of time and with a significant reduction in costs.

2 CALCULATIONS

The harmonic drive analysis involved determining the deformation of the flexspline caused by the wave generator. The calculation was performed using the finite element method in Abaqus. Computational models were created in a computer aided design (CAD) program, based on previous geometric calculations. Since one of the

calculation stages was to assess the impact of torque on the deformation of the flexspline, it was decided to use complete models of all elements of harmonic drive. However, they have been simplified by removing some chamfers, holes, or roundings. This was changed only in those places where the changes introduced did not affect the accuracy of the results obtained. The model of the generator was divided along its minor axis and in the initial phase of calculations its parts were moved separately by the value of w_0 required for proper meshing, causing the required deformation of the flexspline. This stage of the calculation was not considered in the analysis. The deformed flexspline meshes with the circular spline on their major axis. In the minor axis of the generator, the teeth of the two gears pass each other. Meshing occurs only near the major axis of the wave generator for many pairs of teeth at the same time. The rotation of the wave generator causes the meshing of successive pairs of teeth, which causes mutual rotation of the wheels and transmission of torque. In the next step of the calculation, a torque of T = 10 Nm was applied to the circular spline in the reference point defined on the main axis of harmonic drive. The circular spline was linked to the reference point by a rigid link and had all degrees of freedom locked except for rotation around its main axis.Through the teeth located in the meshing area, this load was transferred to the flexspline. Due to this, it was possible to observe the effect of the load on the change in the form of deformation of the body of the flexspline. Also, the authors' knowledge [18, 19] obtained during bench tests showed that too high a load on the harmonic drive caused damage to its elements made of polymer materials with using RP methods. In the calculations, a relatively small torque value was applied, which resulted from the included materials and the assumed use of harmonic drive in the positioning mechanism. It was also assumed that during the work of the harmonic drive, the standing element was a flexspline, fixed at its bottom.

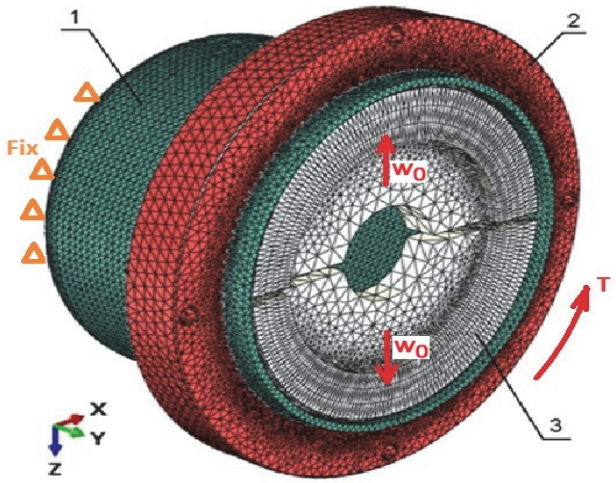

Figure 2 Harmonic drive model after the discretization process; 1 - flexspline, 2 - circular spline, 3 - wave generator

All models of harmonic drive have made a discretization process using tetragonal 10 node quadratic elements (C3D10R). This type of elements was necessary due to the complicated shape in some parts of the models, and the desire to maintain one type of elements for all solids. The mesh nodes were extra compressed on the toothed rim and all contact surfaces between the elements. This was done in accordance with the authors' previous experience, which indicates that discretization with a density of ten square elements at tooth height gives sufficient accuracy with an uncomplicated tooth profile [20]. Finally, more than 800000 finite elements were created for the analyzed computational model in the discretization process, of which 374000 for the flexspline, 325000 for the circular spline and 127000 for the wave generator. The same calculation models were used in all calculations for different materials. In each of the examined cases, only material parameters were changed.

For the calculations were included four materials used in rapid prototyping techniques for production of functional prototypes. Polyamide PA 2200 was chosen as the material used in the SLS method, while ABS was chosen for the FDM method. The resins used in the next methods are FullCure 720 for the JS method and SL5220 for stereolithography (SLA). For these materials, the relevant physical properties were adopted on the basis of manufacturers' catalogues [14, 15] and entered as data for FEM calculations. For example, their Young's modulus values respectively were for PA 2200 E = 1700 MPa, ABS E = 2200 MPa, FullCure 720 E = 2870 MPa, and for SL5220 E = 2700 MPa. It was assumed that the calculations covered the range of elasticity of materials according to Hooke's law and included the nonlinear effect of large displacements.

3 RESULTS

The numerical calculations gave an extensive database of results on various aspects of the work of the analysed harmonic drives. Because the analysis concerns the deformation of the flexspline, only these results will be discussed in the publication. Fig. 3 shows the result of the numerical calculation in the form of a deformation map on the flexspline model. Appropriate colours are indicated by specified displacement values of the finite element nodes. The graphical presentation of the results confirms that the most loaded element of the harmonic drive is the flexspline. Clearly, on its surface there are visible areas of deformation, initially cylindrical sleeve.

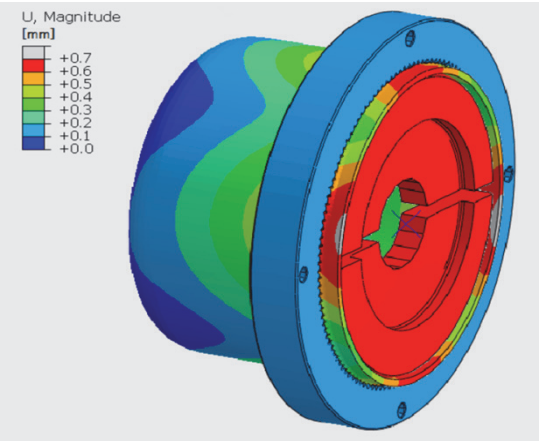

Figure 3 Map of displacements on the harmonic drive model as a result of FEM calculations

The circular spline has a unity blue colour resulting from only its rotation, without deformation. At the same time, the generator model has a uniform red colour. That means the whole model moves as a uniform solid by a value equal to the maximum radial deformation of the flexspline in the large axis of the generator.

The results presented in Fig. 3 are useful for the overall assessment; however, for full control of the results, it is necessary to compare the values in selected places. Since the largest displacement values were located in the major and minor axes of the generator, the model division planes were also positioned there. On the cross sections, the results along the paths marked "A" and "B" next in Fig. 4 and Fig. 5 were read. The start was on the edge of the flexspline from the side of the toothed rim (marked "0"). The displacement graphs for the next nodes of the finite element grid are presented in Fig. 4 and Fig. 5. The displacement values for the major and minor axes of the generator are presented separately. On each of the graphs, the results obtained for the four tested polymeric materials were compared. In all analyzed calculation cases, the graph forms, both for the major and minor axes of the generator, are almost the same whatever the material used. In the minor axis, the displacement graphs have a form similar to linear, while in the major axis, the initial part of the graph is flattened. This area is located in the width of the toothed rim and the wave generator interacting on the flexspline. The free deformation of the flexspline is also limited from the outside by the mating toothed rim of the circular spline. In a minor axis, there is only deformation by the generator, while the teeth of the flexspline and circular spline pass with the clearance, so they do not cause additional deformation. The comparison of the results concerning only deformations did not show important differences, so the radial deformation of the body of the flexspline results only from the interaction of the wave generator, and does not depend on the tested material.

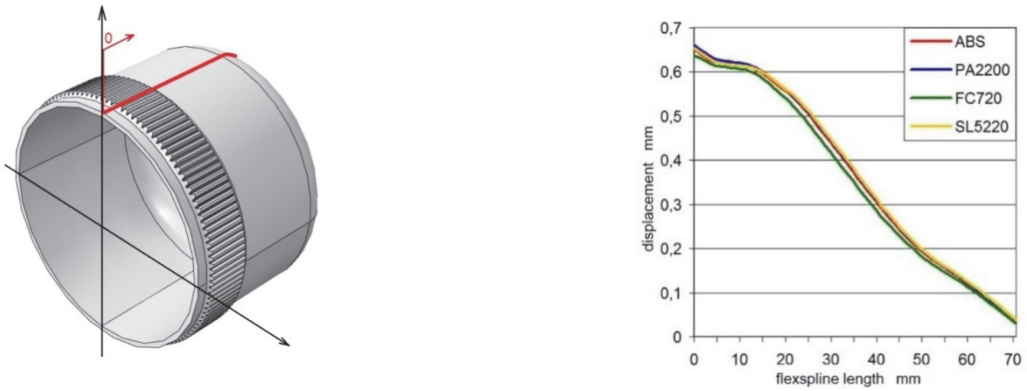

Figure 4 Radial displacements of the flexspline along a major axis

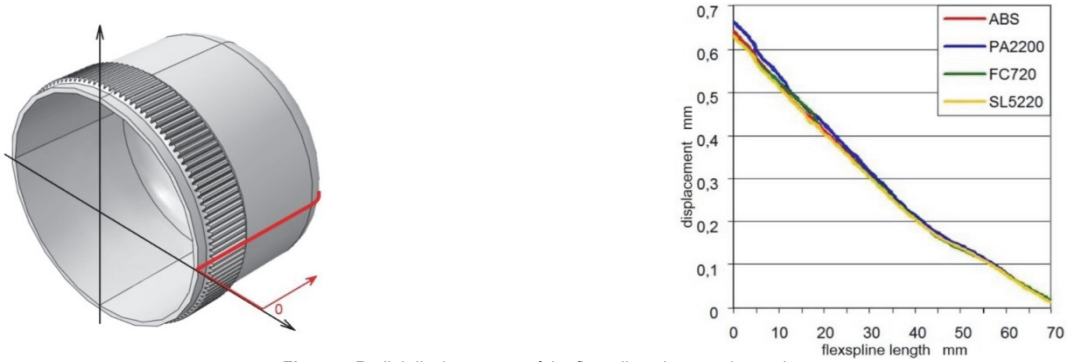

Figure 5 Radial displacements of the flexspline along a minor axis

The next part of the analysis concerned the comparison of the deformation of the flexspline only deformed by the generator, with the same after additional load. To check how the transmitted torque impacts the form of the flexspline sleeve deformation, the results for both computational models were compared. In Fig. 6 to Fig. 9, the radial displacement values for all materials analyzed are presented, read on a cross section passing through a major axis. On each of the graphs there are displacements for the flexspline only deformed and after applying the load. Additional bar charts have also been prepared near the horizontal axis, which show the difference between these results. Due to the small increase in displacement on the body of the flexspline after its load, the obtained values of the deformation change were multiplied 10 times. The greatest impact of the load on the deformation of the flexspline can be observed on the fragment from the toothed rim to the central part of the body sleeve. This is due to the work of the flexspline and circular spline in the mating area. The teeth of the circular spline control the position of the toothed rim of the flexspline, enforcing its specific displacement. The additional displacement observed in the middle of the length of the body is caused by the relative rotation of the toothed rim and the fixed bottom of the flexspline. The flexspline made of FullCure720 resin was the most susceptible to deformation forced by the torque. In this case, in the middle part of the sleeve, the deformation after loading increased more than

5%. The lowest impact of the transferred load was observed in the SL5220 resin, for which the increase was about 1.25%.

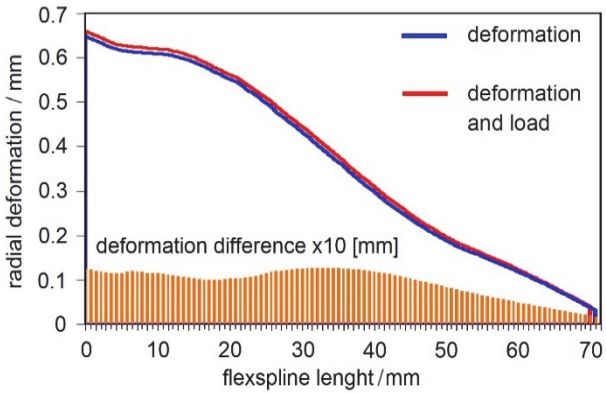

Figure 6 Radial displacement on the major axis of the flexspline for PA 2200

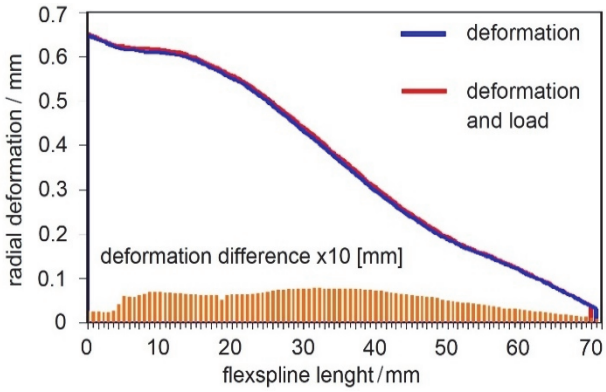

Figure 7 Radial displacement on the major axis of the flexspline for ABS

In a minor axis, a change in deformation is also observed due to the load on the harmonic drive, but of a different character. Due to the out of support, the largest differences in deformation are at the edge of the flexspline near the toothed rim. However, they do not have a decisive impact on the strength of the flexspline, so it will not be discussed in more detail. Radial displacements occurring in a minor axis also do not affect the kinematic accuracy of the harmonic drive, because in this area the teeth of both gears do not mesch. The values of additional deformations directly impact the overall kinematic accuracy of harmonic drive. When designing a wave gear for precision applications, choose a material solution that is not exposed to too much deformation of the thin-walled flexspline body. Therefore, the FullCure720 resin used in the JS method should be eliminated from the analyzed materials.

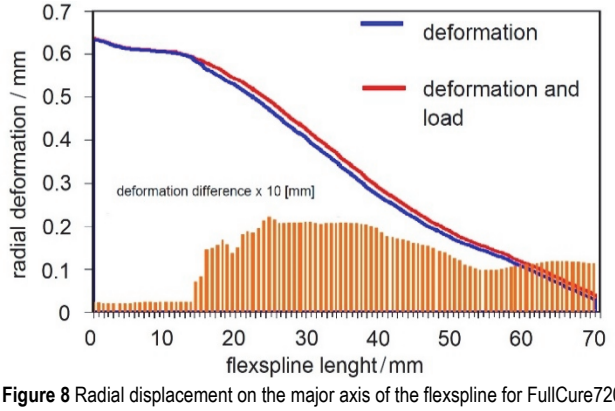

Figure 8 Radial displacement on the major axis of the flexspline for FullCure720

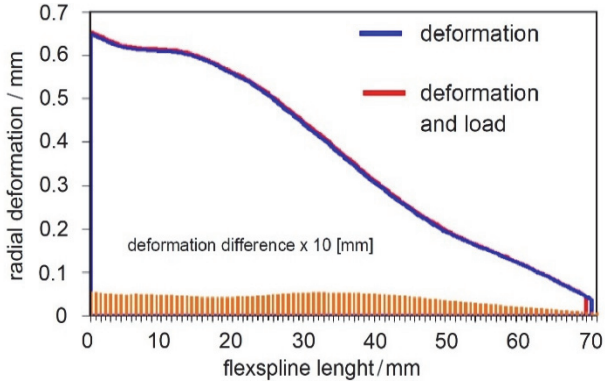

Figure 9 Radial displacement on the major axis of the flexspline for SL 5220

During work, the flexspline body is multidirectionally deformed, but for the correctness of tooth mashing, the most important is the correct shape of the deformation of the toothed rim. To determine it precisely, it is necessary to calculate the displacements of specific points lying on the inert layer of the flexspline under the toothed rim. The values of the radial displacements w, circumferential v, and angle rotation q of the normal line to the neutral layer of the flexspline body at any point for the cam generator can be determined analytically [1, 21-23]. Tab. 1 includes the formulas for determining these parameters with respect to the center of the flexspline, for the angle of rotation of the generator of $\varphi = (0 \div \pi/2)$. However, such calculations are based on simplifications and only allow one to define the profile of the cam generator. The toothed rim is replaced in them by a ring, and the additional load from the teeth is not taken into calculations.

Table 1 Relationships for calculating radial displacements w, and circumferential v and the angle rotation q of the normal line to the neutral layer of the flexspline body; where: w_0 - maximum radial displacement

cam generator	
for	$w = w_0 \cos 2\varphi$
$0 \le \varphi \le \frac{\pi}{2}$	$v = -\frac{w_0}{2} \sin 2\varphi$
	$\theta = \frac{3w_0}{2R} \sin 2\varphi$

Thanks to the numerical calculations of FEM, it is possible not only to calculate the theoretical form of deformation of the flexspline but also to determine the changes in its shape due to the load on the gear. In addition, it is possible to influence the values of the applied moment and observe the effects of these actions on the model of the flexspline.

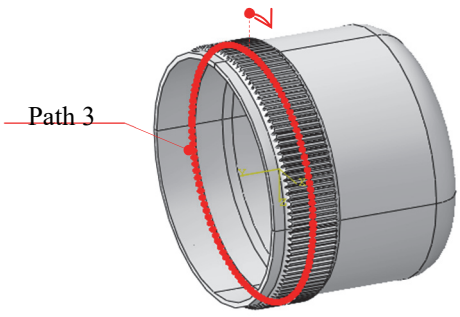

Figure 10 Method of defining the measuring path, for deformation analysis of the flexspline

Various material parameters can also be taken into the calculation and their impact on the load capacity of the harmonic drive can be investigated, as was done in this part of this analysis. It was checked, so what effect on the form of deformation of the toothed rim has the material from which the flexspline was made. In the computational model, the first cross section was defined, passing through the center of the toothed rim, as shown in Fig. 10.

On this plane there were nodes located in the middle of all toothed spaces around the circumference of the flexspline. The beginning of path "C" was located on a major axis of the flexspline, and the next spaces were sequentially numbered in the direction opposite to the torque. The same numbering was defined for the description of the horizontal axis in the graph created for the values read in all calculation models. Fig. 11 shows the values of the displacements of the toothed rim under an impact of load 10 Nm, for the four different materials included in the calculation. These graphs were combined with a graph of deformation that results only from the generator influence without load. A line was also drawn for the theoretical values of the displacements, which were calculated according to the formulas given in Tab. 1. For all materials analyzed, the form of deformation of the loaded flexspline differs significantly from that which is only the result of contact with the generator. In addition, the results calculated in the FEM analysis vary from the theoretical form of deformation. The largest differences are located near a minor axis, because in the deformation profile obtained by the simplified formulas more parameters are not taken into account, for example the material properties of the flexspline. Very clearly the differences are located in the area of a minor axis, where there is no meshing of the teeth of both gears of the harmonic drive. In the toothing area of the circular spline and flexspline, i.e. on a major axis, the graphs have a course similar to the theoretical form of deformation, respectively, for all materials. For the tested polymers, the highest values of additional displacements caused by the load were near a minor axis. Resins are more rigid, because they more accurately preserved the form of deformation of the flexspline obtained earlier only as a result of the operation of the generator.

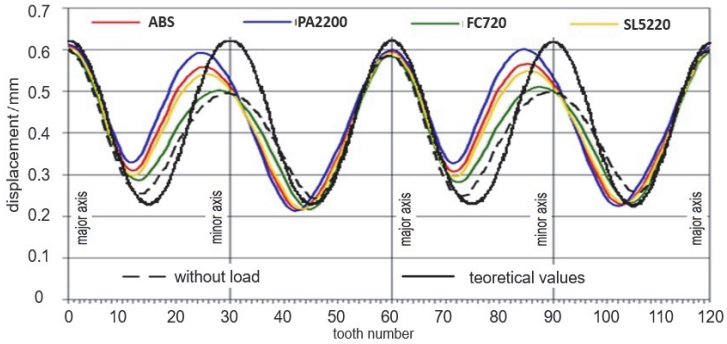

Figure 11 Radial displacement of the toothed rim of the flexspline for different materials

Fig. 12 shows the effect of the added load on the flexspline of the harmonic drive. The first to be shown is a deformed flexspline as a result of contact with a cam generator. The presented form of deformation is the result of numerical calculations of FEM for a model made of ABS polymer. To improve the readability of the presentation, the deformation value of the model was multiplied 10 times compared to the results obtained in the FEM calculations. The first model was only deformed by the generator, a second one which was additionally loaded of torque, applied by a circular spline. The difference in the deformation form of both models is very clear, and what is important, the nature of the changes matches the theoretical descriptions presented in the publications [24, 25]. After loading the flexspline, its evident buckling occurs, and the form of deformation loses symmetry in reference to the main axes. Therefore, it is very important to carefully analyze the form of the deformation of the flexspline during work, and also the effect of the load on its change. The use of rapid prototyping methods for the production of components of harmonic drive often obliges the use of materials of lower strength. The impact of the load on the main elements of the harmonic drive can be deciding to their strength, as shown in the analyzed examples.

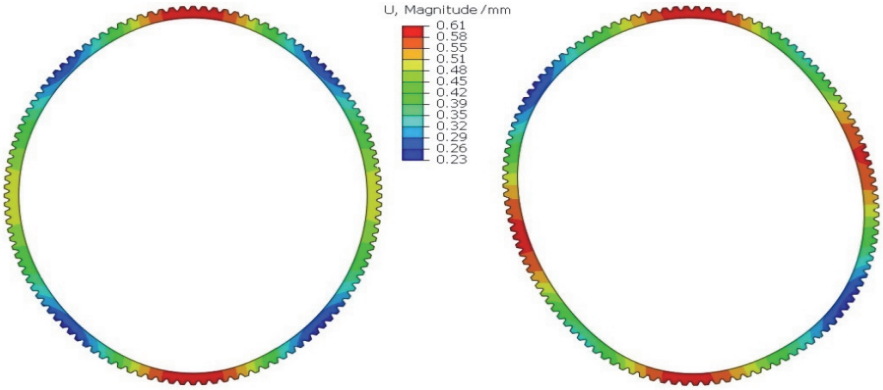

Figure 12 Cross section of the toothed rim of the flexspline for the ABS polymer model: a) deformed by the wave generator, b) deformed and loaded, (scaled x10)

4 SUMMARY

Incremental rapid prototyping methods differ significantly in technology or quality of the manufactured products, but all have some common qualities, because of which they still grow in popularity. Most often, they allow for quick and cheap production of a prototype that meets functional requirements. In their production, direct operator operation is often not required and the models are manufactured on one machine, in an automated manner. Of course, incremental methods also have disadvantages and limitations, but many of them can be repaired through another processing, by considering their requirements during the designing technology. The biggest benefit or sometimes a constraint in the many additive methods is the material used to produce physical models. Prototypes can be manufactured from various materials, but polymers, metals, technical ceramics, wood, rubber, or composites on a metallic or polymer matrix are mainly used [26-29]. However, the accuracy of making elements using RP methods is so high that they can be used in manufacturing processes of even geometrically complicated machine elements. Therefore, an analysis of the possibility of using selected additive methods for the production of a harmonic drive was made. Because polymers have limited strength, it was assumed that the finished prototype would be used in the positioning system of the spacecraft's transmitting antenna. Due to the minimum gravity, the device will work with a limited load, and this was included in the calculations. All of the models analyzed concerned the same design solution and differed only in the material from which they were made. This allowed a comparative analysis to be performed on the possibility of using different polymer materials for harmonic drives. When selecting the materials included in the calculations, the possibility of using them in the manufacture of machine elements by additive methods was taken into account. The deformation of the flexspline by the wave generator obtained very similar results for all models. The deformation did not depend on the material used, but was the result of the defined body shape of the flexspline. Differences were observed between the form of deformation that occurs on the major and minor axis. This is the result of the forced position of the toothed rim of the flexspline bounded inside by the generator and outside by the circular spline. In the next step, it was checked whether the load on the harmonic drive affects the form of deformation of the flexspline. The torque was added to the circular spline, and through the tooth in the meshing area, it was transferred to the flexspline. This resulted in an additional displacement of all cross sections of the flexspline body. The influence of torque for all computational models was most visible on the toothed rim and the central part of the sleeve body. The lower stiffness was characterized by FullCue 720 resin. The model made of SL5220 resin proved to be the least susceptible to additional load. The accuracy of the work of the harmonic drive is determined by the area of tooth cooperation, therefore, the next step of the analysis refers to the toothed rim. In computational models, the results of the displacement of nodes located in the cross section defined in the middle of the width of the toothed rim of the gear of the flexspline were read. The prepared graph showed large discrepancies between the theoretical form of the deformation and the shape of the flexspline obtained in FEM calculations. It should be assumed that the form of deformation obtained in numerical calculations is more similar to the real situation, because it includes not only the deformation due to the wave generator, but also the meshing of the teeth of both wheels and the torque load. Fig. 12 shows the form of deformation of the flexspline only deformed and after its loading. So it is possible to compare how much the torque changes the form of deformation, which has a principal impact on the work quality of the harmonic drive. The use of additive methods indeed increases the options of using harmonic drives, also due to the materials from which they can be made. Rapid prototyping techniques enable remote production of models in environments that are unaccessible to humans. The accuracy of the models made is sufficient for many technologies, and the nature of the work of harmonic drive compensates for the eventual imprecisions. The limitations are mainly due to the strength of the materials used in additive methods, but rapid progress is being made in this field. The repeatability of the shape of the body deformation and the convergence of the results regarding the form of deformation of the toothed rim allows the positive evaluation of most of the analysed models. Of all the polymers, the PA 2200 polyamide was the best. The FullCare 7200 resin showed the lowest torsional stiffness among other materials. On the basis of the analysis, it is possible to positively rate the possibility of using additive methods in the production of harmonic drives made of polymeric materials. However, these technologies should only be used in drives where high kinematic accuracy is required and there are no heavy loads.

5 REFERENCES

[1] Mijał, M. (1999). *Synthesis of wave toothed gears*. Publishing house of the Rzeszów University of Technology: Rzeszow.

[2] Han, B., Chen, Y., Li, H., &Yang, L. (2013). Discrete Model Reference Adaptive Control for Gimbal Servo system of Control Moment Gyro with Harmonic Drive. *Mathematical Problems in Engineering*. https://doi.org/10.1155/2013/897579

[3] Xinjie, Z. & Changxiang, Y. (2010) Application of precision harmonic gear drive in focusing mechanism of space camera, *Proceedings of the SPIE*7659*, 5th International Symposium.* https://doi.org/10.1117/12.866749

[4] Korzynski, M. & Pacana, A. (2010). Centreless Burnishing and Influence of Its Parameters on Machining Effects. *Journal of Materials Processing Technology, 210*(9), 1217-1223. https://doi.org/10.1016/j.jmatprotec.2010.03.008

[5] Pacana, A., Czerwinska, K., & Bednarova, L. (2019). Comprehensive improvement of the surface quality of the diesel engine piston. *Metalurgija, 58*(3-4), 329-332.

[6] Korzynski, M., Dzierwa, A., Pacana, A., & Cwanek, J. (2009). Fatigue strength of chromium coated elements and possibility of its improvement with ball peening. *Surface & Coatings Technology, 204*(5), 615-620. https://doi.org/10.1016/j.surfcoat.2009.08.049

[7] Poklemba, R., Duplakova, D., Zajac, J., Duplak, J., Simkulet, V., & Goldyniak, D. (2020). Design and Investigation of Machine Tool Bed Based on Polymer Concrete Mixture. *International Journal of Simulation Modelling, 19*(2), 291-302. https://doi.org/10.2507/IJSIMM19-2-518

[8] Javernik, A., Buchmeister, B., & Ojstersek, R. (2022). Impact of Cobot parameters on the worker productivity:

Optimization challenge. *Advances in Production Engineering & Management, 17*(4), 494-504. https://doi.org/10.14743/apem2022.4.451

[9] Neuenfeldt-Junior, A., Cheiram, M., Eckhardt, M., Scheuer, C., Siluk, J., & Francescatto, M. (2021). Additive and Subtractive Rapid Prototyping Techniques: A Comparative Analysis of FDM & CNC Processes. *International Journal of Industrial Engineering and Management, 12*(4), 262-273. https://doi.org/10.24867/IJIEM-2021-4-293

[10] Polanec, B., Kramberger, J., & Glodez, S. (2020). A review of production technologies and materials for manufacturing of cardiovascular stents. *Advances in Production Engineering & Management, 5*(4), 390-402. https://doi.org/10.14743/apem2020.4.373

[11] Li, J., Wang, J., Zhou, G., Pu, W., & Wang, Z. (2015). Accelerated life testing of harmonic driver in space lubrication. *Proceedings of the Institution of Mechanical Engineers, Part J: Journal of Engineering Tribology, 229*(12), 1491-1502. https://doi.org/10.1177/1350650115586032

[12] Johnson, M. & Gehling, R. (2006). Head ray life test failure of harmonic gears in a two-axis gimbal for the mars reconnaissance orbiter spacecraft. *Proceedings of the Proceedings of the 38th Aerospace Mechanisms Symposium*, 1-14.

[13] Ueura, K. & Slatter, R. (1999). Development of the harmonic drive gear for space applications. *Proceedings of the 8th European Space Mechanisms and Tribology Symposium,* 438.

[14] Harmonic Drive Systems Inc. Product catalogue. (2017). Speed Reducer Harmonic Drive® Engineering Data.

[15] Reducer catalogue. (2022). Harmonic Drive LLC. Precision Actuators, Gearheads, Gearing Components.

[16] Eisen, H. J., Buck, C. W., Gillis-Smith, G. R., & Umland, J. W. (1997). Mechanical Design of the Mars Pathfinder Mission. *Proceedings 7th European Space Mechanisms and Tribology Symposium*, 293-301.

[17] Hareesh, Y. S. & Varghese, J. (2015). Design and Analysis of Flex Spline with Involute Teeth Profile for Harmonic Drive Mechanism. *International Journal of Engineering Research,* 4. https://doi.org/10.17577/ijertv4is120629

[18] Pacana, J. & Markowska, O. (2016). The analysis of the kinematic accuracy of the actual harmonic drive on a test bench. *Advances in Manufacturing Science and Technology, 40*(01), 47-54.

[19] Pacana, J. & Oliwa, R. (2019). Use of rapid prototyping technology in complex plastic structures Part I. Bench testing and numerical calculations of deformations in harmonic drive made from ABS copolymer. *Polimery/Polymers, 64*(1), 56-65. https://doi.org/10.14314/polimery.2019.1.7

[20] Budzik, G. & Pacana, J. (2008).Analysis of the correctness of the FEM solution depending on the type and number of finite elements used. *Acta Mechanica Slovaca, 3-A*, 327-332.

[21] Dudley D.W. (1962). *Harmonic Drive Arrangements*. Gear Handbook. McGraw-Hill publishing Co., New York.

[22] Mahanto B. S., Sahoo V., & Maiti R. (2018). Effect of Cam Insertion on Stresses in Harmonic Drive in Industrial Robotic Joints. *Procedia Computer Science, 133*, 432-439. https://doi.org/10.1016/j.procs.2018.07.053

[23] Ostapski, W. (2011). *Harmonic drives*. Publishing house of the Warsaw University of Technology: Warsaw 2011.

[24] Ivanov, M. (1987). *The Harmonic Drive*. Defense Industry Press: Beijing.

[25] Ostapski, W. (1998). Engineering Design of harmonic Drive Gearings Towards Quality Criteria. *Machine Dynamics Problems*, 21, 7-159.

[26] Hofmann, D. C., Polit-Casillas, R., Roberts, S. N., Borgonia, J.-P., Dillon, R. P., Hilgemann, E., Kolodziejska, J., Montemayor, L., Suh, J.-O., Hoff, A., Carpenter, K., Parness, A., Johnson, W. L., Kennett, A., & Wilcox, B. (2016). Castable Bulk Metallic Glass Strain Wave Gears: Towards Decreasing the Cost of High-Performance Robotics. *Scientific Reports, 6*. https://doi.org/10.1038/srep37773

[27] Folega, P. & Siwiec, G. (2012) Numerical analysis of selected materials for flexsplines. *Archies of Metallurgy and Materials, 57*(1), 185-191. https://doi.org/10.2478/v10172-012-0008-5

[28] Oh, S. H., Chang, S. H., & Lee D. G. (1997). Improvement of the dynamic properties of a steel-composite hybrid flexspline of a harmonic drive. *Composite Structure, 38*, 251-260. https://doi.org/10.1016/S0263-8223(97)00060-3

[29] Pacana, J. & Oliwa, R. (2019). Use of rapid prototyping technology in complex plastic structures Part II. Impact of operating conditions on functional properties of polymer harmonic drives. *Polimery/Polymers, 64*(3), 216-223. https://doi.org/10.14314/polimery.2019.3.7

Contact information:

Jacek PACANA, PhD, Eng.
Rzeszow University of Technology,
Aleja Powstancow Warszawy 12, 35-959 Rzeszow, Poland
E-mail: pacanaj@prz.edu.pl

Andrzej PACANA, PhD, Eng.
(Corresponding author)
Rzeszow University of Technology,
Aleja Powstancow Warszawy 12, 35-959 Rzeszow, Poland
E-mail: app@prz.edu.pl